

# BRAF V600E-mutated diffuse glioma in an adult patient: a case report and review

Yuta Suzuki<sup>1</sup> · Junko Takahashi-Fujigasaki<sup>2</sup> · Yasuharu Akasaki<sup>1</sup> · Satoshi Matsushima<sup>3</sup> · Ryosuke Mori<sup>1</sup> · Kostadin Karagiozov<sup>1</sup> · Tatsuhiro Joki<sup>1</sup> · Satoshi Ikeuchi<sup>1</sup> · Masahiro Ikegami<sup>4</sup> · Yoshinobu Manome<sup>5</sup> · Yuichi Murayama<sup>1</sup>

Received: 17 July 2015 / Accepted: 24 September 2015 / Published online: 7 October 2015  
© The Japan Society of Brain Tumor Pathology 2015

**Abstract** Recent advances in genomic technology and genome-wide analysis have identified key molecular alterations that are relevant to the diagnosis and prognosis of brain tumors. Molecular information such as mutations in isocitrate dehydrogenase (*IDH*) genes or 1p/19q co-deletion status will be more actively incorporated into the histological classification of diffuse gliomas. *BRAF* V600E mutations are found frequently in circumscribed low-grade gliomas such as pleomorphic xanthoastrocytoma (PXA) and extra-cerebellar pilocytic astrocytoma, or epithelioid glioblastomas (E-GBM), a rare variant of GBM. This mutation is relatively rare in other types of diffuse gliomas, especially in adult onset cases. Here, we present an adult onset case of *IDH* wild-type/*BRAF* V600E-mutated diffuse glioma, evolving from grade III to grade IV. The tumor displayed atypical exophytic growth and had unusual histological features not fully compatible with, but indicative of PXA and E-GBM. We discuss differential diagnosis of

the tumor, and review previously described diffuse gliomas with the *BRAF* V600E mutation.

**Keywords** Anaplastic astrocytoma · Glioblastoma · BRAF mutation

## Introduction

Diffuse gliomas are primary central nervous system tumors, classified as grade II, III and IV by the World Health Organization (WHO) [1]. Grade II and III gliomas often recur and tend to progress to higher grade gliomas, eventually to secondary glioblastoma (GBM). Recent advances in genomic technology and genome-wide analysis have identified key molecular alterations that are relevant to the diagnosis and prognosis of glial tumors [2–5]. Adult onset diffuse gliomas have highly frequent mutations in the isocitrate dehydrogenase (*IDH*) 1 or 2 genes [4, 6–8]. *IDH* mutations are typically accompanied by 1p/19q co-deletions or by *TP53* mutations in mutually exclusive manner. The status of the 1p/19q co-deletion and *TP53* mutation are significantly related to the clinical outcome of *IDH*-mutated diffuse gliomas [9–11]. Wild-type *IDH* diffuse gliomas, accounting for around one-fifth of the diffuse gliomas, have a poorer outcome compared to mutated *IDH*-type gliomas [12].

*BRAF* point or fusion mutations are also driver mutations in glial and glioneuronal tumors, especially in pediatric onset cases [13–18]. The majority of *BRAF* mutations are missense mutations at amino acid position 600 that change a valine into a glutamate (*BRAF* V600E) [17, 19, 20]. The mutated *BRAF* protein is constitutively activated and enhances proliferation potential through the MAPK/ERK signaling pathway [15–17, 19, 20]. *BRAF* V600E is

✉ Junko Takahashi-Fujigasaki  
jnkfuji.0529@gmail.com

<sup>1</sup> Department of Neurosurgery, The Jikei University School of Medicine, Tokyo, Japan

<sup>2</sup> Department of Neuropathology, Brain Bank for Aging Research, Tokyo Metropolitan Institute of Gerontology, 35-2 Sakae-cho, Itabashi-ku, Tokyo 173-0015, Japan

<sup>3</sup> Department of Radiology, The Jikei University School of Medicine, Tokyo, Japan

<sup>4</sup> Department of Pathology, The Jikei University School of Medicine, Tokyo, Japan

<sup>5</sup> Division of Molecular Cell Biology, Core Research Facilities for Basic Science, The Jikei University School of Medicine, Tokyo, Japan

frequently found in pleomorphic xanthoastrocytoma (PXA), ganglioglioma (GG) and extra-cerebellar pilocytic astrocytoma [17, 21, 22]. Previous reports indicated that *BRAF* V600E is also associated with epithelioid GBM (E-GBM), a rare variant of GBM [23–27]. In contrast, *BRAF* V600E mutations are reported to be rare in diffuse gliomas [12, 17].

Here, we present a rare case of a wild-type *IDH/BRAF* V600E-mutated diffuse glioma, progressing to GBM. We discuss differential diagnosis of the tumor, and review previously reported diffuse glioma cases with the *BRAF* mutation.

## Clinical summary

A 37-year-old woman was admitted to our hospital with left hemiparesis and homonymous hemianopia. Her past medical history, including epilepsy, was negative. A slightly hyper-dense mass without cysts and calcifications was found by computed tomography (CT) scans in the right temporal lobe (Fig. 1a). Magnetic resonance imaging (MRI) revealed a lobulated 6.0 × 6.0 cm lesion in the right temporal lobe with nearly homogenous enhancement that extended exophytically into the supra- and retrosellar space (Fig. 1b–d). When removed, the tumor had an intra-axial origin, growing exophytically around the brain stem, and tended to engulf cranial nerves and major vessels. After subtotal removal of the tumor, conventional radiotherapy and chemotherapy with temozolomide were performed. Seventeen months after the first operation, the patient was re-operated because of recurrence. The tumor had the same characteristics as when operated the first time and was subtotally resected. In addition, the patient underwent cyber knife radiosurgery and immunotherapy. Her state of consciousness and physical status gradually deteriorated, and she died from pneumonia 2 years after reoperation.

## Pathological findings

The tumor had an infiltrative margin, and was mainly composed of plump, round eosinophilic cells with short processes (Fig. 1e, f). Cells with scant cytoplasm and elongated thin processes were also present. Nuclei of the plump cells were occasionally hyperchromatic with prominent nucleoli, and were located eccentrically. A small number of multinucleated cells were also present. Some of these cells contained small- to medium-sized vacuoles (Fig. 1g). A few eosinophilic granular bodies were found (Fig. 1h). There was perivascular lymphocytic cuffing (Fig. 1e), but without increased reticulin fiber deposition, pseudopalisading necrosis and microvascular proliferation. Mitotic rates were 5 per 10 high power fields. The

immunohistochemical study was performed with a Ventana XT system (BenchMark<sup>®</sup> XT; Ventana Medical Systems, Inc., Tuscon, AZ, USA). Sections for nestin, IDH1-H and IDH1-S were probed with primary antibodies diluted in Immuno Shot Mild (Cosmobio, Tokyo, Japan) and were immunostained using the Histofine Simple Stain MAX-PO kit (Nichirei, Tokyo, Japan). INI1 was probed with the EnVision<sup>™</sup> System (DAKO Corporation, Carpinteria, CA, USA). The tumor cells were positive for GFAP (Fig. 1i); the cytoplasm of the plump cells was particularly well stained. Expression of nestin, S100 protein and vimentin was strong and diffuse. Many of the tumor cells contained CD34 immunoreactivity (Fig. 1j). The MIB-1 LI was 9.2 % in the main area. The results of the immunohistochemical analysis are summarized in Table 1.

The histological features of the tumor were similar after both resections. The number of tumor cells with enlarged hyperchromatic nuclei and scant cytoplasm increased (Fig. 1k). A higher degree of nuclear pleomorphism was noted, and the multinucleated cells increased in number. There was microvascular proliferation and small foci of necrosis at the periphery of the section. Mitotic figures increased up to 12 mitoses per 10 high power fields. Expression of GFAP was generally decreased compared to the first surgical specimens. The MIB-1 LI peaked at 19 % in the high cellular areas. Expression of CD34 was diffuse in almost all areas. It was observed in differentiated astrocytic, small immature and pleomorphic cells, but became weak in hypercellular areas of the second resection. The tumor cells in both resections were partially positive for neuronal markers such as synaptophysin (<10 %), neurofilament (<3 %) and chromogranin A (<30 %, and generally weak). The tumor was weakly but diffusely positive for p16 and EGFR. Expression of INI1 was preserved in the tumor cells.

Genetic study revealed a *BRAF* V600E mutation in the initial surgical material. No mutations in exon 4 of *IDH1* and *IDH2* were found. DNAs were extracted from paraffin-embedded sections. Specimens were deparaffinized, followed by proteinase K digestion (Sigma Aldrich, 10 mg/sections), and extracted DNAs were subjected to amplification (Perkin Elmer 9700). The primers for *BRAF* were F 5'-TGCTTGCTCTGATAGGAAAATG-3' and R 5'-CCACAAAATGGATCCAGACA-3' (exon 15, NM\_004333), for *IDH1* were F 5'-AATGAGCTCTATATGCCATCACTG-3' and R 5'-AATCACATTATTGCCAACCATGACTTACTTG-3' (exon 4, NM\_005896 in GenBank), and for *IDH2* were F 5'-ATCCCACGCCTAGTCCCTGGCTGGACC AAG-3' and R 5'-CAGAGACAAGAGGATGGCTAGGC GAGGAGC-3' (exon 4, NM\_002168). Products were directly sequenced on a 3730xl DNA Analyzer (Applied Biosystems, Foster City, CA) with the Big Dye Terminator v3.1 Cycle Sequencing Kit (Applied Biosystems).

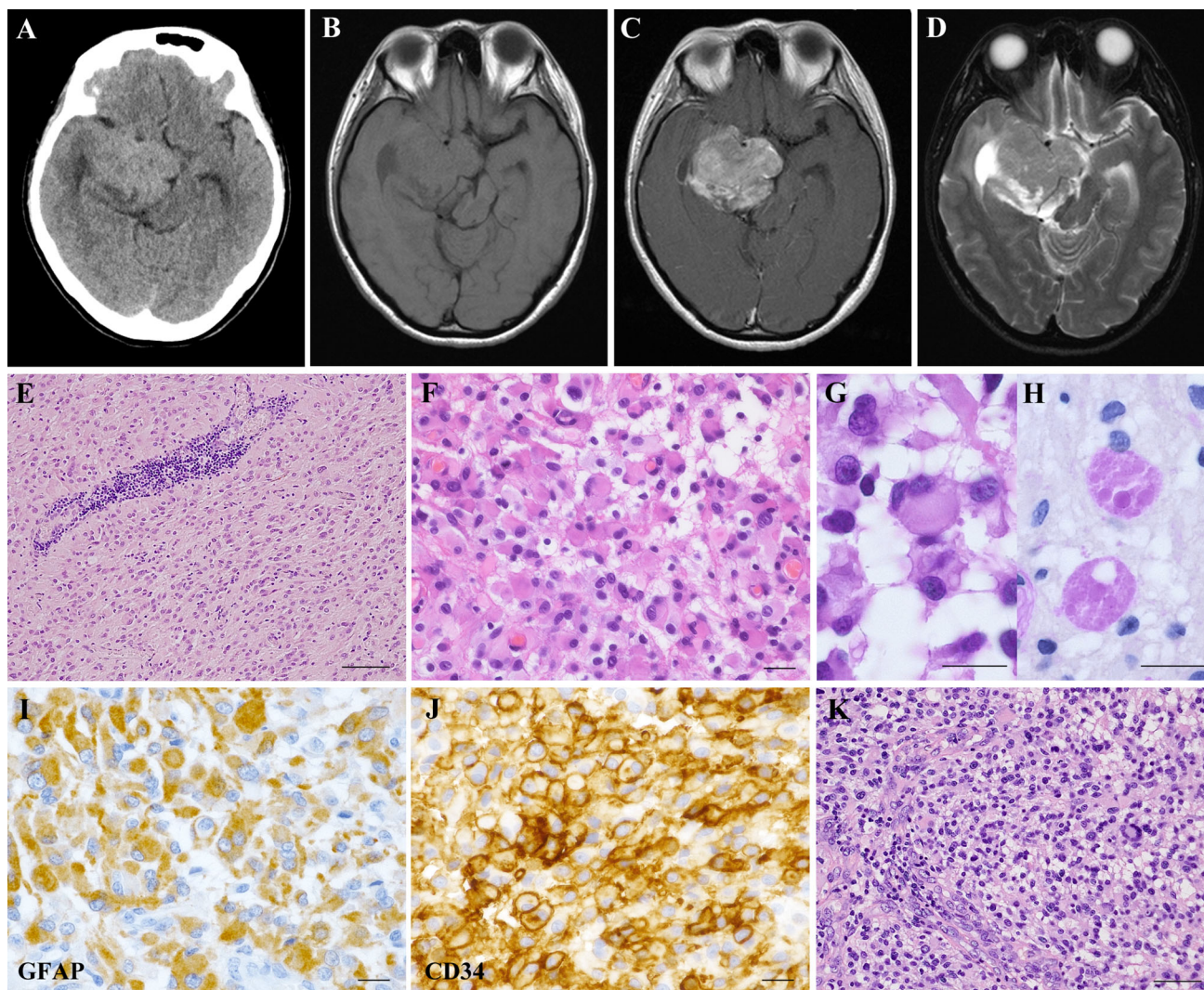


**Fig. 1** Computed tomography (CT) scans and magnetic resonance images (MRI) taken before the first operation (**a–d**). The tumor was slightly hyper-dense on CT scans (**a**), slightly low-intensity on T1-weighted images (**b**), T1-weighted gadolinium-enhanced MRI revealed a nearly homogenous enhanced mass, without regions of poor contrast enhancement (**c**), slightly high-intensity on T2-weighted images (**d**). Pathological features of the tumor after the first resection (**e–j**). The plump, eosinophilic cells with short processes proliferated

diffusely, and perivascular lymphocytic cuffing was observed (**e, f**). Tumor cells with small to medium sized vacuoles and PAS-positive eosinophilic granular bodies were present (**g, h**). The tumor cells were positive for GFAP (**i**) and CD34 (**j**). After the second resection, the tumor showed increased cellularity and pleomorphism with microvascular proliferation (**k**). **e–g, k** Hematoxylin and eosin. **h** Periodic acid-Schiff stain. **i** Immunohistochemistry (IHC) for GFAP. **j** IHC for CD34. **e, k** Bar 50  $\mu$ m. **f–j** Bar 20  $\mu$ m

## Discussion

The tumor displayed atypical radiographic features; its growth was apparently exophytic and it had well-demarcated borders. Pathologically, the tumor consisted of GFAP-positive cells with abundant cytoplasm and short stellate processes or scant cytoplasm with elongated processes. Mitotic rates were high, and the tumor was diagnosed as a Grade III anaplastic astrocytoma (WHO classification 2007) [1]. However, the tumor had some specific features. There was a small but not negligible number of multinucleated cells with vacuolated

cytoplasm. The presence of a few eosinophilic granular bodies, perivascular cuffing and CD34 immunoreactivity suggested that the tumor shared some pathological characteristics with circumscribed gliomas such as PXA or GG. The tumor cells expressed neuronal markers, synaptophysin, NF and chromogranin A with variable frequency. These cells were morphologically indistinguishable from other astrocytic cells, and not taken to be neuronal components.

It is still debatable whether the tumor should be categorized as a circumscribed/localized astrocytoma. Histological examination of circumscribed gliomas often shows

**Table 1** Immunohistochemical profile in the tumor

	GFAP	Vim	S-100	Nestin	Olig2	Syn	NF	Chromo	CD34	CK	EMA	P16	EGFR	INI1	p53 (%)	Ki-67 (%)	IDH1-H	IDH1-S
First	+	++	++	++	+	±	±	±	+	-	-	+	+	+	18	9.2	-	-
Second	±	++	++	++	+	±	±	±	+	-	-	+	+	+	20	19	-	-

*GFAP* glial fibrillary acid protein (DAKO, rabbit, polyclonal), *Vim* vimentin (novocastra, mouse, clone V9), *S-100* (DAKO, rabbit, polyclonal), *Nestin* (IBL, rabbit, polyclonal), *Olig2* (IBL, rabbit, polyclonal), *Syn* synaptophysin (novocastra, rabbit, clone 27G12), *NF* neurofilament (DAKO, mouse, clone 2F11), *Chromo* chromogranin A (DAKO, mouse, clone DAK-A3), *CD34* (BD Biosciences, mouse, clone My10), *CK* cytokeratin (BD Biosciences, mouse, clone CAM 5.2), *EMA* epithelial membrane antigen (DAKO, mouse, clone E29), *p16* (abcam, rabbit, clone EPR 1473), *EGFR* (novocastra, mouse, clone EGFR.113), *INI1* (Abnova, mouse, clone 3E10), *p53* (novocastra, mouse, clone DO-7), *Ki-67* (DAKO, mouse, clone MIB-1), *IDH1-H* (DANOVA, mouse, clone H09), *IDH1-S* (IBL, mouse, clone SMab-1)

an infiltrative margin as in the present case. The most important differential diagnosis for this case is PXA with anaplastic features. The tumor lacked the classical features of PXA: proliferation of spindle cells with fascicular patterns and a reticular formation. Basically, the tumor was composed of fibrillary or gemistocytic astrocytic cells. Pleomorphism was not prominent; only a small number of vacuolated cells and eosinophilic granular bodies were detected by careful re-evaluation. Anaplastic astrocytomas rarely, but can show exophytic growth [28]. Taking these pathological features into consideration, we tentatively diagnosed the tumor as an anaplastic astrocytoma. Chi et al. [29] reported 7 adult cases of *BRAF*-mutated diffuse gliomas with atypical radiographic and histological features. They described the gliomas as infiltrating, but with relatively well-demarcated borders, similar to the tumor we described here. The atypical histological features described by the authors included the presence of ependymal-like cells, proliferation of spindle tumor cells into subarachnoid and Virchow-Robin spaces, and piloid growth of tumor cells with Rosenthal fibers. Although the atypical pathological features mentioned by the authors were not necessarily compatible with those of our case, it should be noted that *BRAF*-mutated diffuse gliomas have somewhat “unusual” histological features.

The *BRAF* V600E mutation is rare in diffuse gliomas, but certain number of cases has been reported [12, 16–19, 22–27, 29–51]. Through a literature search, total 113 diffuse gliomas were listed (Table 2): 38 cases of grade II, 14 cases of grade III including 2 gliomatosis cerebri, 54 cases of grade IV, 2 cases of grade II–III, and 5 case of grade III–IV. When available, age and gender of the patients, location of the tumor, *IDH1* mutation and 1p/19q status were recorded in the table. As previously reported, the *BRAF* V600E mutation was found preferentially in young patients; 56 patients were 20 years of age or under. Pediatric gliomas and glioneuronal tumors have molecular backgrounds that differ from adult tumors [18, 48]. *IDH* mutations, a major mutation in adult grade II and III diffuse gliomas, are rare in pediatric gliomas [16, 18, 50]. *BRAF* V600E mutations were found in 23 % of low-grade diffuse astrocytomas in a large cohort of low-grade pediatric gliomas [18]. Ramkissoon et al. [43] also reported a similar frequency of *BRAF* V600E mutations in diffuse pediatric astrocytomas; however, this mutation is rare in diffuse adult gliomas, in which the prevalence is estimated at less than 1 % [12].

Affected females seemed to predominate in the listed tumors (39 female, 29 male cases); however, the gender of the other 45 cases was unknown. Most commonly, *BRAF*-mutated diffuse gliomas arise from the cerebral cortex; the temporal and temporo-parietal lobes seem to be most frequently affected (19 cases).

**Table 2** The previously reported BRAF mutation in gliomas

Type	BRAF mutations	Age (year)	Gender	Location	IDH1	1p/19q	Other information	References
DA	MacConaill et al. [34]	Pediatric					Astrocytoma WHO Grade II	[34]
	Sievert et al. [35]	13	F	Bithalamic				[35]
	Schiffman et al. [16]	19		Brain stem			DLGA, CDKN2A (D)	[16]
		20		Occipital			DLGA, CDKN2A (D)	
	Kim et al. [39]	1 Case		Temporal	+		A598 V	[39]
	Chi et al. [29]	41	F	Rt. parietal				[29]
		30	F	Rt. temporal				
		22	F	Lt. temporal				
		28	M	Rt. temporal				
	Ramkissoon et al. [43]	1.4	F	Forebrain				[43]
		5.6	M	Forebrain				
		8.3	F	Forebrain				
		13	M	Forebrain				
	Zhang et al. [18]	3	M	Cerebral cortex				[18]
		3	M	Cerebral cortex				
		3	F	Cerebral cortex				
		9	M	Cerebral cortex				
		10	F	Diencephalon				
	Roth et al. [47]	11	M				An indeterminate subtype LGG	[47]
OA	Gierke et al. [48]	3 Pediatrics (0–18)						[48]
OG	Chi et al. [29]	32	F	Lt. temporal		-		[29]
	Jeuken et al. [32]	1 Case					V600 M	[32]
	Schindler et al. [17]	39	M	Lt. temporal	-	-		[17]
	Myung et al. [41]	53			+	+		[41]
	Badiali et al. [37]	1 Case			-	-		[37]
	Kim et al. [39]	1 Case		Rt. occipital	-	L		[39]
DA, OG, NOS	Horbinski et al. [38]	Pediatric		Cerebellum				[38]
LGG	Korshunov et al. [49]	1	F	Midline	-			[49]
		1	M	Midline	-			
		11	M	Hemispheric	-			
		7	F	Hemispheric	-			
LGG-NOS	Ramkissoon et al. [43]	10.2	F	Cerebellum				[43]
		10.6	M	Forebrain				
		10.2	F	Brain stem				

Table 2 continued

Type	BRAF mutations	Age (year)	Gender	Location	IDH1	1p/19q	Other information	References
AA	Schiffman et al. [16]	10.2 15.8	M F	Forebrain Forebrain				[16]
	Schiffman et al. [16]	13		Temporal			CDKN2A (D)	
AO	Schindler et al. [17]	5 13		Frontal Cerebellum				[17]
	Lin et al. [40]	Pediatric		Pediatric				[40]
G2-3 glioma	Myung et al. [41]	1 Case						[41]
	Myung et al. [41]	35	F		+	-		[41]
		39	F		+	-		
		50	M		-	-		
		53	F		-	-		
		45	M		+	+		[41]
GC	Badiali et al. [37]	1 Case			+	+		[37]
	Suzuki et al. [12]	Adults 2 cases			+	+		[12]
C-GBM	Schindler et al. [17]	77	F	Lt. temporal with spread in frontal and occipital	-	-		[17]
	Fernandez-Vega et al. [45]	67	F	Brain stem and cerebellar hemispheres	-	-	Involving cerebral hemisphere and spinal cord V599E	[45]
C-GBM	Knobbe et al. [30]	Adults 2 cases						[30]
	Basto et al. [31]	46 41						[31]
C-GBM	Hagemann et al. [33]	1 Case						[33]
	Schiffman et al. [16]	17		Parietal			CDKN2A (D)	[16]
C-GBM	Nicolaides et al. [36]	17		Parietal			CDKN2A (D)	[36]
	Schindler et al. [17]	6 Cases 2 Pediatrics						[17]
C-GBM	Myung et al. [41]	46	F		-	-	Progressed from DA	[41]
	Betegowda et al. [42]	53	M					[42]
C-GBM		17		Rt. temporoparietal				
		18		Rt. temporal				
C-GBM	Chi et al. [29]	Pediatric					1 of additional 6 pediatric GBM	[29]
		23	F	Rt. parietal	-	-		
C-GBM		66	M	Rt. parietal	-	-		
	Bleeker et al. [44]	1 Case						[44]

Table 2 continued

Type	BRAF mutations	Age (year)	Gender	Location	IDH1	1p/19q	Other information	References
	Robinson et al. [46]	9		Rt. frontoparietal	–		CDKN2A (D)	[46]
	Roth et al. [47]	2	M		–		Progressed from LGG	[47]
	Mistry et al. [50]	Pediatric, 9<	M	Hemispheric	–		Progressed from LGG	[50]
		Pediatric, 9<	M	Hemispheric	–		CDKN2A (D), Progressed from PA	
		Pediatric, 9<	M	Hemispheric	–		CDKN2A (D), Progressed from PXA	
		Pediatric, 9<	M	Hemispheric	–		CDKN2A (D), Progressed from LGA	
		Pediatric, 9<	M	Hemispheric	–		Progressed from LGA [CDKN2A (D)]	
		Pediatric, 9<	F	Midline	–		Recurrence after 22 months	[51]
	Takahashi et al. [51]	49	M	Rt. parietooccipital	–			[51]
E-GBM	Kleinschmidt-DeMasters et al. [23]	27	F	Lt. occipital	–			[23]
		43	M	Lt. temporoparietal	–			
		10	F	Rt. parietooccipital	–			
		29	M	Lt. temporal	–			
		21	F	Rt. temporal	–			
		29	F	Lt. temporoparietal	–			
		50	M	Lt. temporal	–			
		10	F	Thalamus	–			[24]
		11	M	Temporal	–			
		10	F	Bithalamic	–			
	Nobusawa et al. [25]	22	M	Rt. occipital	–			[25]
	Tanaka et al. [26]	25–26	F	Lt. temporal	–		Progressed from PXA	[26]
	Kleinschmidt-DeMasters et al. [27]	55	M	Lt. temporal	–			[27]
		39	F	Lt. frontal	–			
		32	F	Rt. parietal	–			
		69	M	Lt. parietal	–			
R-GBM	Myung et al. [41]	20	F		–			[41]

Table 2 continued

Type	BRAF mutations	Age (year)	Gender	Location	IDH1	1p/19q	Other information	References
GC-GBM	Schindler et al. [17]	22	F				Progressed from DA	[17]
	Dias-Santagata et al. [22]	30	F	Lt. temporal			Progressed from PXA	[22]
HGG	Myung et al. [41]	1 Case 36	F		-	-		[41]
	MacConaill et al. [34]	Pediatric	F		-	-		[34]
	Korshunov et al. [49]	8	F	Midline	-	-		[49]
		13	F	Midline	-	-		
		7	F	Midline	-	-		
Gliosarcoma	Knobbe et al. [30]	1 Case	F	Midline	-	-	V599E	[30]
	Schindler et al. [17]	32			-	-		[17]

DA diffuse astrocytoma, OA oligoastrocytoma, OG oligodendroglioma, NOS not otherwise specified, LGG low-grade glioma, AA anaplastic astrocytoma, AO anaplastic oligodendroglioma, G2-3 glioma grade II and III gliomas, GC gliomatosis cerebri, C-GBM classical glioblastoma, E-GBM epithelioid GBM, R-GBM rhabdoid GBM, GC-GBM giant cell GBM, HGG high grade glioma, f female, m male, rt. right, lt. left, IDH1+ mutation, IDH1- no mutation, 1p/19q+ co-deletion, 1p/19q- no co-deletion, L 1p/19q loss, DLGA diffuse infiltrating low-grade astrocytoma, CDKN2A (D) CDKN2A deletion, LGA low-grade astrocytoma, Ref. reference number, blank not in detail

Among the grade II and III gliomas, 34 cases were astrocytic, 7 cases were oligodendrocytic, one case was oligoastrocytic; the other 12 cases were unspecified. An *IDH1* mutation was detected in 6 of the 50 cases investigated: 1 case of diffuse astrocytoma (DA), 2 cases of anaplastic astrocytoma (AA), 1 case of oligodendroglioma (OG) and 2 cases of oligodendroglioma (AO). One case of *IDH*-mutated OG and 2 cases of AO had concomitant 1p/19q co-deletions. Thus, *IDH* mutations, 1p/19q co-deletions and *BRAF* V600E mutations are not necessarily mutually exclusive [37, 41]. The 3 gliomas harboring these three molecular events contained oligodendrocytic components. Neither *IDH* mutations nor 1p/19q co-deletions were found in the grade IV glioblastomas. Of note, 10 cases of *BRAF*-mutated diffuse astrocytomas had deletions of *CDKN2A*, known to be found frequently in PXA [52], and all cases were 20 years of age or under [16, 47, 50]. Recent reports indicated that secondary pediatric high grade gliomas with *BRAF* mutation and *CDKN2A* deletion arose from low-grade counterparts after long latency, and showed favorable clinical outcomes compared to GBMs without these molecular alterations [49, 50].

A close association between *BRAF*V600E mutations and E-GBM has been reported. The other types of grade IV glioblastomas than E-GBM are also associated with this type of mutation (Table 2). Some of the *BRAF*-mutated GBMs, with both classical and variant histology, progressed from preexisting low-grade gliomas [17, 22, 26, 50], as in our case. Kleinschmidt-DeMasters et al. [23] examined 13 E-GBM, 2 Rhabdoid GBM (R-GBM) and 9 Giant cell GBM (GC-GBM) cases, and identified *BRAF* V600E mutations in 7/13 (54 %) E-GBMs, but not in R-GBMs or GC-GBMs. E-GBM, a rare morphological variant of glioblastoma, was not yet defined in the 4th edition of WHO classification in 2007. E-GBMs are composed of patternless sheets of “melanoma-like” epithelioid cells with round eosinophilic cytoplasm and eccentrically located nuclei. These cells are discohesive and devoid of stellate cellular processes [53–55]. In our case, eosinophilic round cells, somewhat resembling epithelioid cells, proliferated. However, the cells generally had short thin stellate processes (Fig. 1f, g). When the tumor progressed to Grade IV, tumor cells with faint cytoplasm predominated (Fig. 1k). Large, round mono- or multinucleated eosinophilic cells were also present. These cells were not “melanoma-like”, but resembled the atypical glial cells in classical GBMs. We considered that the histological features of our case were not necessarily compatible with those of E-GBM. As discussed above, the tumor shared some pathological characteristics with PXA. A case of E-GBM arising from PXA was previously reported [26]. Very recently, Alexandrescu et al. reported a series of PXA cases with anaplastic foci resembling E-GBM [56].



Importantly, these cases were strongly associated with *BRAF*V600E mutations. Our case had histological features not fully compatible with, but indicative of, PXA and E-GBM. Clear histological definition of PXA-E-GBM lineage tumors will be needed for accurate classification of tumors harboring pathological features that are difficult to interpret, as in our case.

R-GBM is also a rare variant that shares some overlapping morphological features with E-GBM [23, 55]. GC-GBM is composed of bizarre, multinucleated giant cells, with occasional reticulin deposits; it was defined as a subtype of GBM in the WHO classification [1]. Histological definitions of these rare subtypes have not been clearly established yet, and these variants are often confused. Inactivation of *INI1* is considered to be associated with rhabdoid tumor cells, and focal loss of *INI1* protein has been proposed to be an important indicator for the diagnosis of R-GBM [23, 55, 57]. *INI1* expression was not examined in all of the cases. Careful re-evaluation will be needed to clarify how the molecular alteration, *BRAF* mutation, *INI1* inactivation and other molecular events that have not yet been evaluated, relate to the histological variants of GBMs.

Our patient survived 2 years after the diagnosis of GBM and multimodal treatments. Some reports indicated that *BRAF* V600E mutations might be a favorable prognostic factor in adult GBMs with classical histology [29, 58]. In contrast, E-GBMs, in which *BRAF* mutations are frequent, are known to have an aggressive clinical behavior [24, 26]. The prognostic significance of *BRAF* mutations in diffuse gliomas should be addressed through longer follow-up of large glioma cohorts. From now on, molecular information with prognostic, predictive and therapeutic value will be actively incorporated into the histological classification of brain tumors. Importantly, the *BRAF* V600E mutation can be a therapeutic target in glial tumors [14, 36, 46]. Therefore, to find this molecular alteration efficiently, further elucidation of the clinico-pathological features of *BRAF*-mutated diffuse gliomas will be necessary.

**Acknowledgments** We thank Dr. M Ruberg for a critical reading of the manuscript, Drs. Shinji Ito and Dr. Takashi Komori for the immunohistochemistry, and the latter for kind advice concerning the diagnosis.

## References

- Louis D, Ohgaki H, Wiestler O et al (2007) WHO classification of tumours of the central nervous system, 4th edn. International Agency for Research on Cancer, Lyon
- Cairncross G, Berkey B, Shaw E et al (2006) Phase III trial of chemotherapy plus radiotherapy compared with radiotherapy alone for pure and mixed anaplastic oligodendroglioma: intergroup Radiation Therapy Oncology Group Trial 9402. *J Clin Oncol Off J Am Soc Clin Oncol* 24:2707–2714
- van den Bent MJ, Carpentier AF, Brandes AA et al (2006) Adjuvant procarbazine, lomustine, and vincristine improves progression-free survival but not overall survival in newly diagnosed anaplastic oligodendrogliomas and oligoastrocytomas: a randomized European Organisation for Research and Treatment of Cancer phase III trial. *J Clin Oncol Off J Am Soc Clin Oncol* 24:2715–2722
- Parsons DW, Jones S, Zhang X et al (2008) An integrated genomic analysis of human glioblastoma multiforme. *Science (New York, NY)* 321:1807–1812
- Weller M, Felsberg J, Hartmann C et al (2009) Molecular predictors of progression-free and overall survival in patients with newly diagnosed glioblastoma: a prospective translational study of the German Glioma Network. *J Clin Oncol Off J Am Soc Clin Oncol* 27:5743–5750
- Bals J, Meyer J, Mueller W et al (2008) Analysis of the *IDH1* codon 132 mutation in brain tumors. *Acta Neuropathol* 116:597–602
- Watanabe T, Nobusawa S, Kleihues P et al (2009) *IDH1* mutations are early events in the development of astrocytomas and oligodendrogliomas. *Am J Pathol* 174:1149–1153
- Yan H, Parsons DW, Jin G et al (2009) *IDH1* and *IDH2* mutations in gliomas. *New Engl J Med* 360:765–773
- Ichimura K, Pearson DM, Kocialkowski S et al (2009) *IDH1* mutations are present in the majority of common adult gliomas but rare in primary glioblastomas. *Neuro Oncol* 11:341–347
- Ohgaki H, Kleihues P (2009) Genetic alterations and signaling pathways in the evolution of gliomas. *Cancer Sci* 100:2235–2241
- Ichimura K (2012) Molecular pathogenesis of *IDH* mutations in gliomas. *Brain Tumor Pathol* 29:131–139
- Suzuki H, Aoki K, Chiba K et al (2015) Mutational landscape and clonal architecture in grade II and III gliomas. *Nat Genet* 47:458–468
- Jones DT, Kocialkowski S, Liu L et al (2008) Tandem duplication producing a novel oncogenic *BRAF* fusion gene defines the majority of pilocytic astrocytomas. *Cancer Res* 68:8673–8677
- Pfister S, Janzarik WG, Remke M et al (2008) *BRAF* gene duplication constitutes a mechanism of *MAPK* pathway activation in low-grade astrocytomas. *J Clin Invest* 118:1739–1749
- Jones DTW, Kocialkowski S, Liu L et al (2009) Oncogenic *RAF1* rearrangement and a novel *BRAF* mutation as alternatives to *KIAA1549: BRAF* fusion in activating the *MAPK* pathway in pilocytic astrocytoma. *Oncogene* 28:2119–2123
- Schiffman JD, Hodgson JG, VandenBerg SR et al (2010) Oncogenic *BRAF* mutation with *CDKN2A* inactivation is characteristic of a subset of pediatric malignant astrocytomas. *Cancer Res* 70:512–519
- Schindler G, Capper D, Meyer J et al (2011) Analysis of *BRAF* V600E mutation in 1,320 nervous system tumors reveals high mutation frequencies in pleomorphic xanthoastrocytoma, ganglioglioma and extra-cerebellar pilocytic astrocytoma. *Acta Neuropathol* 121:397–405
- Zhang J, Wu G, Miller CP et al (2013) Whole-genome sequencing identifies genetic alterations in pediatric low-grade gliomas. *Nat Genet* 45:602–612
- Davies H, Bignell GR, Cox C et al (2002) Mutations of the *BRAF* gene in human cancer. *Nature* 417:949–954
- Wan PT, Garnett MJ, Roe SM et al (2004) Mechanism of activation of the *RAF-ERK* signaling pathway by oncogenic mutations of *B-RAF*. *Cell* 116:855–867
- Dougherty MJ, Santi M, Brose MS et al (2010) Activating mutations in *BRAF* characterize a spectrum of pediatric low-grade gliomas. *Neuro Oncol* 12:621–630

22. Dias-Santagata D, Lam Q, Vernovsky K et al (2011) BRAF V600E mutations are common in pleomorphic xanthoastrocytoma: diagnostic and therapeutic implications. *PLoS One* 6:e17948
23. Kleinschmidt-DeMasters BK, Aisner DL, Birks DK et al (2013) Epithelioid GBMs show a high percentage of BRAF V600E mutation. *Am J Surg Pathol* 37:685–698
24. Broniscer A, Tatevossian RG, Sabin ND et al (2014) Clinical, radiological, histological and molecular characteristics of paediatric epithelioid glioblastoma. *Neuropathol Appl Neurobiol* 40:327–336
25. Nobusawa S, Hirato J, Kurihara H et al (2014) Intratumoral heterogeneity of genomic imbalance in a case of epithelioid glioblastoma with BRAF V600E mutation. *Brain Pathol (Zurich, Switzerland)* 24:239–246
26. Tanaka S, Nakada M, Nobusawa S et al (2014) Epithelioid glioblastoma arising from pleomorphic xanthoastrocytoma with the BRAF V600E mutation. *Brain Tumor Pathol* 31:172–176
27. Kleinschmidt-DeMasters BK, Aisner DL, Foreman NK (2015) BRAF VE1 immunoreactivity patterns in epithelioid glioblastomas positive for BRAF V600E mutation. *Am J Surg Pathol* 39:528–540
28. Tanaka K, Sasayama T, Kawamura A et al (2006) Isolated oculomotor nerve paresis in anaplastic astrocytoma with exophytic invasion. *Neurol Med Chir (Tokyo)* 46:198–201
29. Chi AS, Batchelor TT, Yang D et al (2013) BRAF V600E mutation identifies a subset of low-grade diffusely infiltrating gliomas in adults. *J Clin Oncol Off J Am Soc Clin Oncol* 31:e233–e236
30. Knobbe CB, Reifenberger J, Reifenberger G (2004) Mutation analysis of the Ras pathway genes NRAS, HRAS, KRAS and BRAF in glioblastomas. *Acta Neuropathol* 108:467–470
31. Basto D, Trovisco V, Lopes JMM et al (2005) Mutation analysis of B-RAF gene in human gliomas. *Acta Neuropathol* 109:207–210
32. Jeuken J, van den Broecke C, Gijzen S et al (2007) RAS/RAF pathway activation in gliomas: the result of copy number gains rather than activating mutations. *Acta Neuropathol* 114:121–133
33. Hagemann C, Gloger J, Anacker J et al (2009) RAF expression in human astrocytic tumors. *Int J Mol Med* 23:17–31
34. MacConaill LE, Campbell CD, Kehoe SM et al (2009) Profiling critical cancer gene mutations in clinical tumor samples. *PLoS One* 4:e7887
35. Sievert AJ, Jackson EM, Gai X et al (2009) Duplication of 7q34 in pediatric low-grade astrocytomas detected by high-density single-nucleotide polymorphism-based genotype arrays results in a novel BRAF fusion gene. *Brain Pathol (Zurich, Switzerland)* 19:449–458
36. Nicolaidis TP, Li H, Solomon DA et al (2011) Targeted therapy for BRAFV600E malignant astrocytoma. *Clin Cancer Res Off J Am Assoc Cancer Res* 17:7595–7604
37. Badiali M, Gleize V, Paris S et al (2012) KIAA1549-BRAF fusions and IDH mutations can coexist in diffuse gliomas of adults. *Brain Pathol (Zurich, Switzerland)* 22:841–847
38. Horbinski C, Nikiforova MN, Hagenkord JM et al (2012) Interplay among BRAF, p16, p53, and MIB1 in pediatric low-grade gliomas. *Neuro Oncol* 14:777–789
39. Kim Y-HH, Nonoguchi N, Paulus W et al (2012) Frequent BRAF gain in low-grade diffuse gliomas with 1p/19q loss. *Brain pathology (Zurich, Switzerland)* 22:834–840
40. Lin A, Rodriguez FJ, Karajannis MA et al (2012) BRAF alterations in primary glial and glioneuronal neoplasms of the central nervous system with identification of 2 novel KIAA1549:BRAF fusion variants. *J Neuropathol Exp Neurol* 71:66–72
41. Myung JK, Cho H, Park C-KK et al (2012) Analysis of the BRAF(V600E) mutation in central nervous system tumors. *Transl Oncol* 5:430–436
42. Bettgowda C, Agrawal N, Jiao Y et al (2013) Exomic sequencing of four rare central nervous system tumor types. *Oncotarget* 4:572–583
43. Ramkissoon LA, Horowitz PM, Craig JM et al (2013) Genomic analysis of diffuse pediatric low-grade gliomas identifies recurrent oncogenic truncating rearrangements in the transcription factor MYBL1. *Proc Natl Acad Sci USA* 110:8188–8193
44. Bleeker FE, Lamba S, Zanon C et al (2014) Mutational profiling of kinases in glioblastoma. *BMC Cancer* 14:718
45. Fernandez-Vega I, Quirk J, Norwood FL et al (2014) Gliomatosis cerebri type 1 with extensive involvement of the spinal cord and BRAF V600E mutation. *Pathol Oncol Res POR* 20:215–220
46. Robinson GW, Orr BA, Gajjar A (2014) Complete clinical regression of a BRAF V600E-mutant pediatric glioblastoma multiforme after BRAF inhibitor therapy. *BMC Cancer* 14:258
47. Roth JJ, Santi M, Rorke-Adams LB et al (2014) Diagnostic application of high resolution single nucleotide polymorphism array analysis for children with brain tumors. *Cancer Genet* 207:111–123
48. Gierke M, Sperveslage J, Schwab D et al (2015) Analysis of IDH1-R132 mutation, BRAF V600 mutation and KIAA1549-BRAF fusion transcript status in central nervous system tumors supports pediatric tumor classification. *J Cancer Res Clin Oncol* 27 [Epub ahead of print]
49. Korshunov A, Ryzhova M, Hovestadt V et al (2015) Integrated analysis of pediatric glioblastoma reveals a subset of biologically favorable tumors with associated molecular prognostic markers. *Acta Neuropathol* 129:669–678
50. Mistry M, Zhukova N, Merico D et al (2015) BRAF mutation and CDKN2A deletion define a clinically distinct subgroup of childhood secondary high-grade glioma. *J Clin Oncol Off J Am Soc Clin Oncol* 33:1015–1022
51. Takahashi Y, Akahane T, Sawada T et al (2015) Adult classical glioblastoma with a BRAF V600E mutation. *World J Surg Oncol* 13:100
52. Weber RG, Hoischen A, Ehrler M et al (2007) Frequent loss of chromosome 9, homozygous CDKN2A/p14(ARF)/CDKN2B deletion and low TSC1 mRNA expression in pleomorphic xanthoastrocytomas. *Oncogene* 26:1088–1097
53. Kleinschmidt-DeMasters BK, Meltesen L, McGavran L et al (2006) Characterization of glioblastomas in young adults. *Brain Pathol (Zurich, Switzerland)* 16:273–286
54. Rodriguez FJ, Scheithauer BW, Giannini C et al (2008) Epithelial and pseudoepithelial differentiation in glioblastoma and gliosarcoma: a comparative morphologic and molecular genetic study. *Cancer* 113:2779–2789
55. Bette Kay K-D, Ali HA, Diane KB et al (2010) Epithelioid versus rhabdoid glioblastomas are distinguished by monosomy 22 and immunohistochemical expression of INI-1 but not claudin 6. *Am J Surg Pathol* 34:341–354
56. Alexandrescu S, Korshunov A, Lai SH et al (2015) Epithelioid glioblastomas and anaplastic epithelioid pleomorphic xanthoastrocytomas—same entity or first cousins? *Brain pathology (Zurich, Switzerland)* bpa.12295. [Epub ahead of print]
57. Shogo E, Shunsuke T, Shigeru Y et al (2013) Primary rhabdoid tumor with low grade glioma component of the central nervous system in a young adult. *Neuropathology* 33:185–191
58. Dahiya S, Emmett RJ, Haydon DH et al (2014) BRAF-V600E mutation in pediatric and adult glioblastoma. *Neuro Oncol* 16:318–319